



## **Performance assesement for ultrasonic testing of austenitic stainless steel welds with finite elements simulation**

Ophélie Salauze<sup>1</sup>

1 EDF Direction Industrielle, France, ophelie.salauze@edf.fr

### **Abstract**

Complex materials like multi-pass welds in austenitic stainless steels greatly disturb the propagation of ultrasonic waves and make ultrasonic non-destructive testing difficult. Such welds show anisotropic and heterogeneous structures, with elongated grains, inducing deviation and/or division of the ultrasonic beam associated with a strong attenuation of wave amplitude.

The ATHENA 2D finite elements simulation code has been developed to simulate ultrasonic propagation in the weld, and to properly reproduce these beam distortion phenomena.

The feasibility study presented in this paper aims at developing and testing a new approach with ATHENA, based on simulation, to evaluate the performance of an ultrasonic inspection in terms of zone coverage and sensitivity. The weld, made by manual shield metal arc welding (SMAW), was modeled, using information extracted from welding notebooks, with the MINA model which predicts columnar grains orientation. Then, the ultrasonic beam was simulated at each scanning position of the probe. The amplitude of the transmitted sound field was computed and compared to the field in the isotropic parent material. The overlay of these beams allowed us to determine the areas of the weld which are not sounded below a given threshold, and to identify areas where the response of a defect is assumed to be weaker. Data compilation obtained with the analysis of the beams calculated in the two scanning directions and with different probes provide additional technical justifications for the evaluation of the performance of ultrasonic testing in austenitic steel welds.

### **1. Introduction**

In-service inspection is a major challenge in the nuclear industry. Ultrasonic techniques are particularly used to ensure components integrity. Nevertheless, ultrasonic inspection is made difficult in the presence of complex materials. Multi-pass welds in austenitic stainless steel present an anisotropic and heterogeneous structure, with large and elongated grains. The impact of such structures on wave propagation is well known. It can generate ultrasonic beam deviation and sometimes even beam division. And the amplitude of ultrasonic waves is strongly attenuated. EDF has developed a finite element code, called ATHENA, which has proven its efficiency to accurately reproduce the complex phenomena above-mentioned (1,2) as long as the weld is properly modelled.

Multi-pass welds made by manual SMAW are difficult to describe due to their anisotropic and heterogeneous properties (grain orientation varies in the full welding volume). The MINA model has been developed in order to calculate the grain local direction in a

realistic manner from the welding process and information present in the welding notebook (3).

The methodology detailed in this paper has been developed to fulfill the requirements of a French performance qualification for defense in depth. Its particularity lies in performance assessment on the zone coverage and on the detection of targeted defects. The goal of this feasibility study is to go further than ray tracings which are commonly used for qualification (simple geometrical reasoning or the approach described in (4)). This methodology has been applied to a case study chosen to be rather disadvantageous regarding ultrasounds perturbation. The 2D version of ATHENA coupled with the MINA model have been used and performances on both zone coverage and sensitivity have been evaluated.

## **2. Numerical modelling**

### ***2.1 ATHENA code***

The ATHENA is a finite element code that simulates ultrasonic wave propagation in all kinds of elastic media such as heterogeneous and anisotropic structures (5,6). It is based on the solving of the elastodynamic equations in the calculation zone. ATHENA enables the simulation of all propagation and interaction phenomena, including the mode conversion phenomena that may cause parasitic echoes. The efficiency of the code relies on the fact that the calculation domain discretization uses a square and regular mesh while defects are described using the fictitious domains method using an independent mesh (6). This method combines the rapidity of regular meshes calculation with the possibility to model arbitrary shaped defects. Furthermore, perfectly matched absorbing layers allow simulation of infinite domains: the addition of absorbent layers removing spurious reflections on artificial edges of the calculation zone. Various inspection configuration can be modelled with a wide range of probes (conventional single-element crystal, TOFD configuration), materials and reflectors.

Wave scattering on grain boundaries is also taken into account in ATHENA, allowing prediction of realistic values of echo amplitudes. A specific model was developed to integrate scattering attenuation laws, especially for anisotropic media (1).

Validation of the software is based on comparisons between simulation results and experimental results obtained on representative mock-ups. The experimental data were obtained from acquisition systems available at EDF R&D. Several projects carried out with ATHENA was related to the ability to inspect austenitic welds with ultrasound. The study of several industrial applications, limited to 2D configurations, has confirmed the validity of the code for dealing with the case of anisotropic and heterogeneous media (1).

### ***2.2 MINA model***

In order to obtain realistic quantitative results in these anisotropic and heterogeneous media, a fine characterization of the columnar grain structure is needed to achieve the weld grain orientation mapping.

The MINA model (3) aims at estimating columnar grain orientation from the knowledge of some parameters specific of the welding process and information extracted from the welding notebook (geometry chamfer, electrode diameter, electrode inclination, number of welding passes and welding sequence).

### 2.3 Case study

The configuration has been chosen in order to be rather disadvantageous regarding sound propagation: the weld presents a large X-chamfer and an important thickness (80 mm). The Figure 1 presents on the left the cartography computed by the MINA model. The informations usually extracted from the notebook have been chosen in order to be representative of a manual SMAW weld. This cartography is then divided into small squares and the average orientation is computed and fed into the ATHENA software (right side of Figure 1).

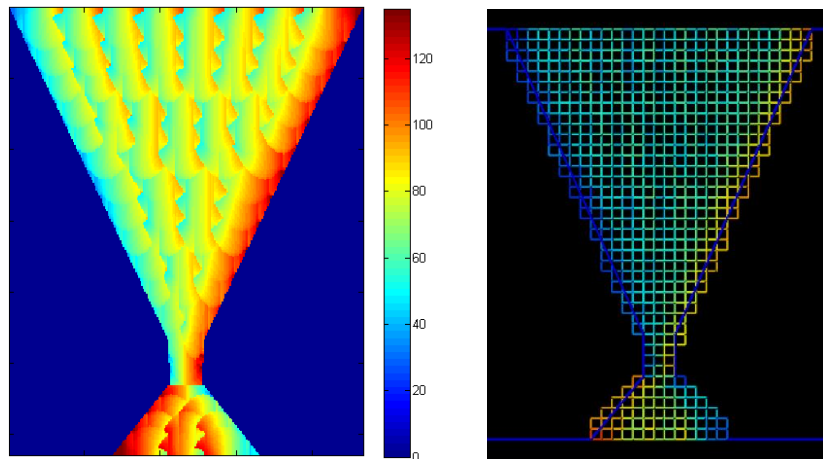


**Figure 1. Weld cartography with grain orientation obtained with MINA model (left: cartography directly computed with MINA; right: average orientations on small squares implemented in ATHENA code)**

Material parameters such as wave propagation speeds, attenuation values (depending on grain orientation) and elastic constant values have been taken from previous studies on austenitic stainless steel materials conducted at EDF R&D.

Three refraction angles have been chosen as test cases: 35°, 45° and 55°. The aperture of transducers is equal to 30 mm and the wave frequency is 2 MHz.

## 3. Methodology for results exploitation

The inspection is performed in the direction perpendicular to the weld, and it has been simulated for the two scanning directions. Results processing is done in three phases: field calculation with ATHENA, field thresholding, and field overlap.

### 3.1 Raw field calculation

The ATHENA code simulates, at each probe position, the ultrasonic wave propagation in the material. For each position, it is also able to compute the transmitted field over the calculation zone. The field calculated by ATHENA is the emission field, i.e. it corresponds to the acoustic pressure of the incident field.

Figure 2 shows the acoustic field computed by ATHENA 2D at different probe position with a refraction angle of 45°. These are raw fields, which are not normalized by a common reference but only by the maximum of amplitude at each position. It can be seen

that the ultrasonic beam is distorted and deflected while crossing the chamfer. Besides, when the probe is entirely over the weld, the beam shape is significantly changed.

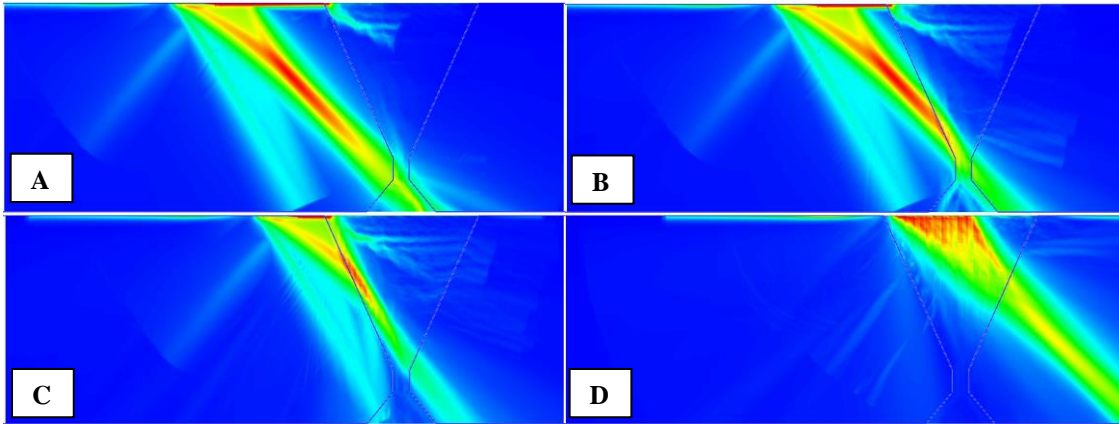


Figure 2. Raw emission fields at different scan positions. Refraction angle of 45°.

### 3.2 Thresholding

The transmitted field is also computed in the isotropic parent material to be used as a reference field. For each probe position and each mesh of the calculation zone, the amplitude of the field is compared to the maximum amplitude of the reference field at the same depth (see the example of Figure 3), by the formula below (the resulting amplitude is thus expressed in decibel). A threshold is also applied which correspond to the equivalent detection threshold.

$$A_{dB} = 10 * \log_{10} \left( \frac{A}{A_{ref}^{max}} \right) \quad (1)$$

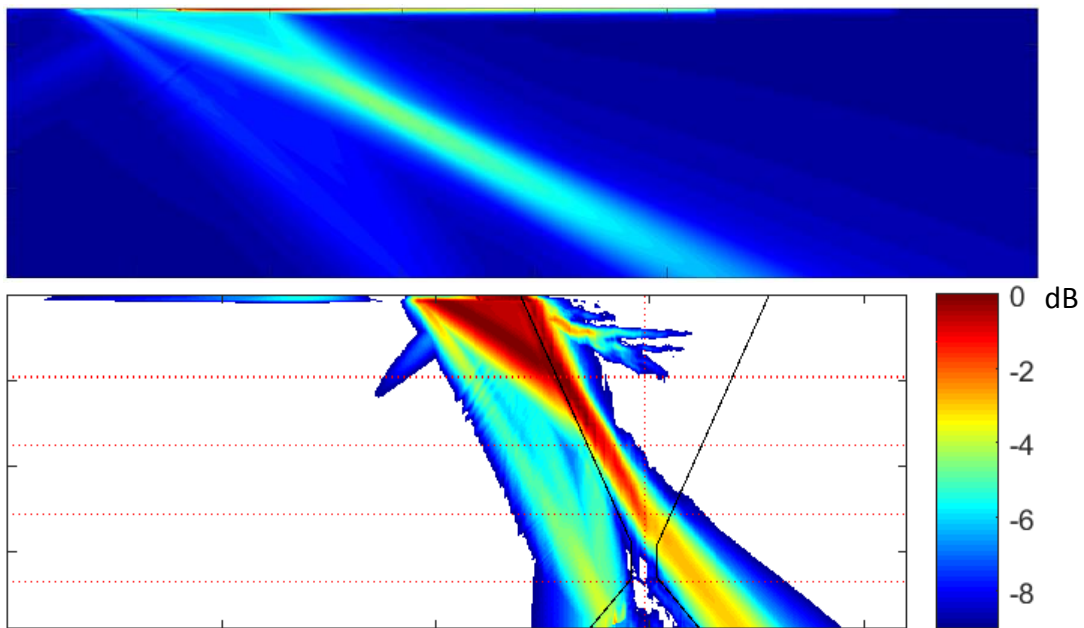


Figure 3. Above: Reference field in parent metal. Below: Computed field normalised by reference field corresponding to the position C on Figure 2. Refraction angle = 45°. Threshold = -9 dB.

The resulting images show the calculation zone areas which are sounded by the ultrasonic field and the corresponding amplitudes. The zones which are not sounded and the zones sounded below the chosen threshold appear in white. In our representation, the colour bar is extended from 0 dB to the threshold: there is no colour differentiation between amplitudes over the reference and amplitudes exactly at 0 dB.

### 3.3 Field overlap

The next step is to overlap all the fields obtained for each probe positions in order to display them on the same image. Thus, the resulting image presents in each point the maximum amplitude obtained during the probe scan. Several probe scans can also be overlapped on the same image.

## 4. Results and discussion

There are two advantages with this kind of representation. Firstly, the zone coverage is given taking into account the complexity of the material (beam deviations and attenuation). Secondly, the resulting results are quantitative and illustrate the performances in terms of sensitivity. It gives an overview of the zones where the response of a defect is assumed to be weaker. And it avoids running numerous numerical simulations and/or experiments with the targeted defect.

### 4.1 Performance assessment on zone coverage

Figure 4 presents the beam overlay for the two scan directions and the compilation of the two directions. The threshold has been fixed at 3 dB, which is equivalent to a detection threshold of 6 dB for defect detection. The compilation of the two scanning directions is shown on Figure 5.

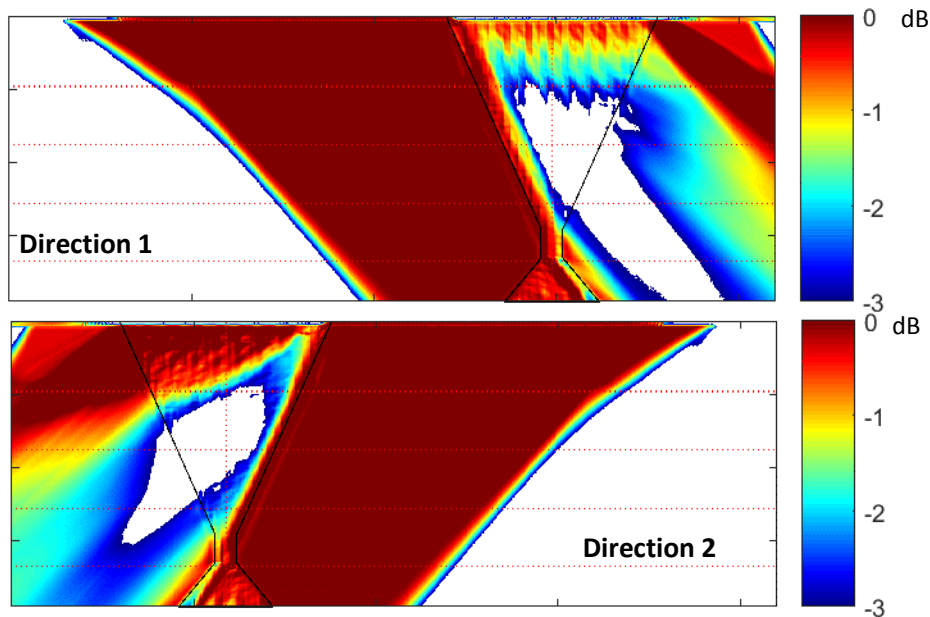


Figure 4. Field overlay for the two scan directions. Refraction angle =  $45^\circ$ . Threshold = -3 dB.

These figures show that, for a 45° refraction angle, the zone which is not sounded is rather significant. And this is especially true when the acoustic beam has to go through the entire welded volume. For both control directions, there is a “blind zone” in the welded volume: a defect would not be detected at this threshold in the welding volume at mid-thickness. In order to be entirely inspected in this configuration, the threshold value would have to be modified.

Besides, in the scanning direction 1, the “blind zone” reaches the inner surface. Consequently, for this configuration an inspection in the two directions would be necessary for inner surface examination.

However, in the case where a planar defect is the targeted defect, some precaution must be taken for interpretation. The analysis presented here does not take into account the orientation of the reflector.

The same analysis has been made with the same detection threshold but with different refraction angles (see Figure 5). With a 35° beam, a larger “blind zone” is observed in the welding volume. On the contrary, with 55° there is no “blind zone”.

The working range of the three probes correspond basically to the second half of the material thickness. In the case of the 35° refraction angle, the images show a strong deviation of the ultrasonic beam resulting in a “blind zone” extended to the whole width of the weld. Consequently, this beam should not be used for the inspection of this weld.

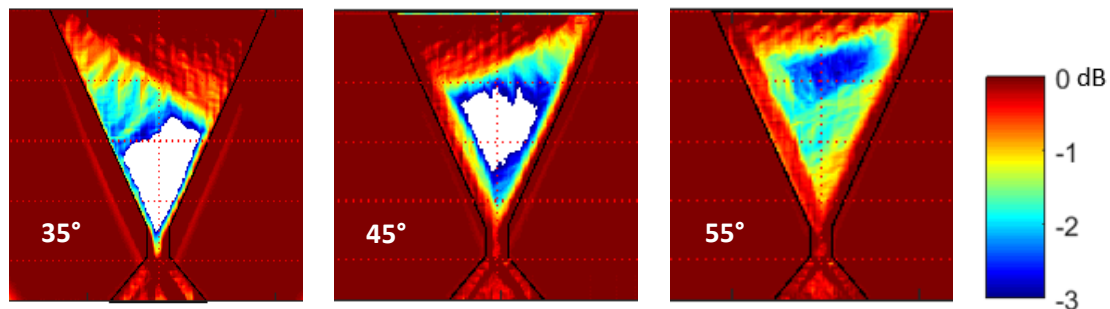


**Figure 5. Field overlays with both directions at the different refraction angles. Threshold = -3 dB.**

As was said before, this assessment of zone coverage can be useful to determine the value of the detection threshold necessary for the inspection. But, austenitic welds are also generate parasitic echoes due to the heterogeneous and isotropic structure. The presence of these parasitic echoes are simulated by the ATHENA code with Bscan simulations. So, a balance has to be found between lowering threshold values while analysing zone coverage representations and limiting the impact of parasitic echoes on the UT analysis.

#### **4.2 Performance assessment on sensitivity**

With this simple visualization, the most penalising configuration in term of detection can be determined. The figures with field overlays are actually an illustration of sensitivity performances on small reflectors (reflectors smaller than the focal spot at the given threshold). This is illustrated with the following sensitivity study on 2 mm diameter side-drilled holes (SDHs).

Table 1 presents the amplitude of the echoes generated by SDHs localized at the weld axis at different depths, for the three refraction angles under study. Table 2 presents the amplitude of SDHs located at different positions at the same depth for the 45° refraction angle. These amplitudes can be obtained either by Bscans calculations with ATHENA

2D, or by the analysis of the fields overlays above. It should be noted that in the second case, amplitudes must be multiplied by two to correspond to the emission/reflection field.

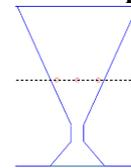
**Table 1. Echoes amplitude generated by SDHs located at the weld axis for the two scanning directions; the amplitudes are compared to the amplitudes of echoes generated by SDHs located into the parent metal at the same depth**

SDH depth	35°		45°		55°	
	Dir. 1	Dir.2	Dir. 1	Dir.2	Dir. 1	Dir.2
40 mm	-19 dB	-15 dB	-11.6 dB	-13.8 dB	-8.3 dB	-5.7 dB
55 mm	-26 dB	-15 dB	-5.3 dB	-7.1 dB	-1.9 dB	-2.9 dB
70 mm	+2.1 dB	-0.3 dB	+1.8 dB	+0.5 dB	+0.6 dB	+2.0 dB



**Table 2. Echoes Amplitude generated by SDHs located at different positions regarding to the weld axis, at 40 mm depth for the 45° refraction angle; the amplitudes are compared to the amplitudes of echoes generated by SDHs located into the parent metal at the same depth**

45° / 40 mm depth	Dir. 1	Dir. 2
Axis	-11.6 dB	-13.8 dB
Axis -10 mm	-1.7 dB	-16 dB
Axis + 10 mm	-14 dB	-3.4 dB



In the study case, the amplitude of the reflector at the weld junction is higher than the reference in the parent material. And the amplitude decreases while depth decreases (see Table 1) due to beam deviation and attenuation of the ultrasonic waves. On the contrary, the amplitude of the echo is higher close to the chamfer than at the weld axis (see Table 2).

If other kinds of defects are targeted, additional simulations would be needed. The above study would have to be performed with the defect located at the areas where defect responses are assumed to be weaker. Then, the Bscan would be calculated with the targeted defect.

## 5. Conclusions

The main objective of this feasibility study was to demonstrate that fields study can provide complementary technical justifications for the assessment of the performance of ultrasonic testing in austenitic steel welds.

Data compilation obtained with the analysis of the ultrasonic beams allows to have many informations on a limited number of images and with a limited number of simulations and experiments. Beam perturbations due to the heterogeneous and anisotropic structure of austenitic steel welds are taken into account to determine zone coverage. And the sensitivity performance can be directly evaluated on resulting images.

Overlap images can be compiled for different scan directions and different probes with their corresponding working ranges and the associated thresholds. On the same figure a qualitative overview of zone coverage (zones sounded at a given threshold) is displayed as well as the quantitative assessment of sensitivity.

This feasibility study also showed that field analysis can be a supporting tool to determine the value of the detection threshold necessary for the inspection. However, this value would have to be confirmed by a Bscan simulation and/or experiments with the targeted defect, especially if the defect is a planar defect. This analysis can also be helpful to reject refraction angles which would not be appropriate for the control.

This feasibility study is very promising to consolidate technical justifications. Now, it has to be applied in a real industrial case for the study of influential parameters.

### **Acknowledgements**

The ATHENA code is being developed by EDF (French Electricity Board) and INRIA (National Research Institute in Computer Science and Automated Systems). MINA model has been developed in collaboration with the Laboratory of Non-Destructive Characterisation (Université de la Méditerranée, Aix en Provence, France). The authors would like to express their gratitude to Mr. Sharfine Shahjahan (EDF Direction Industrielle) for his availability and his help in data processing.

### **References and footnotes**

1. B. Chassignole, V. Duwig, M.-A. Ploix, P. Guy, R. El Guerjouma, “Modelling the attenuation in the ATHENA finite elements code for the ultrasonic testing of austenitic stainless welds”, *Ultrasonics* 49 pp 653-658, 2009
2. B. Chassignole, O. Dupond, L. Doudet, V. Duwig, and N. Etchegaray, “Ultrasonic examination of an austenitic weld: Illustration of the disturbances of the ultrasonic beam”, *Rev. Progr. QNDE* 28 (B) pp 1886-1893, 2008
3. A. Apfel, J. Moysan, G. Corneloup, T. Fouquet, B. Chassignole, “Coupling an ultrasonic propagation code with a model of the heterogeneity of multi-pass welds to simulate ultrasonic testing”, *Ultrasonics* 43 pp 447-456, 2005
4. J.A. Ogilvy, “An alternative ray tracing model for ultrasonic non-destructive testing”, *NDT & E International*, Volume 25, Number 1, 1992
5. E. Becache, P. Joly, C. Tsogka, “An analysis of new mixed finite elements for the approximation of wave propagation problems”, *SIAM Journal of Numerical Analysis* 37 pp 1053-1084, 2000
6. E. Becache, P. Joly, C. Tsogka, “Application of the fictitious domain method to 2D linear elastodynamic problems”, *Journal of Computational Acoustic* 9 pp 1175-1202, 2001